A PHYSICAL MODEL OF CONVECTIVE-DISPERSIVE TRANSPORT IN AN INTERGRANULAR POROUS MATERIAL

A. Rubeša – V. Travaš*

Department of Hydraulic Engineering, Faculty of Civil Engineering, University of Rijeka, Radmile Matejčić 3, Rijeka

ARTICLE INFO

***Article history*:**
Received 17.09.2012.
Received in revised form 16.01.2013.
Accepted 17.01.2013.

Keywords:
Convective-dispersive transport
Darcy law
Mass concentration
Physical modeling
Saturated porous media
Steady seepage flow

Abstract:

A physical model for tracer transport in an intergranular porous material is presented. Particularly, the measured temporal variations of a tracer mass concentration inside the physical model are compared to the one predicted for the same boundary and initial conditions by the 1D and 2D analytical solutions of the governing differential equation. A non-reactive tracer and steady flow conditions are considered. The Péclet number for the considered flow is such that the molecular diffusion can be neglected.

1 Introduction

The importance of studying transport phenomena in porous materials is obvious [1, 2]. However, among all the variety of conditions under which the transport of mass in porous materials can occur [3], the main attention is here dedicated to transport phenomena that are characteristic for groundwater flows [1]. Particularly, the transport of a chemically non-reactive tracer in a fully saturated intergranular aquifer is considered. Under these circumstances, the tracer transport is mainly caused i.e. induced by convection. In other words, the velocity vectors of the water contained in the intergranular aquifer are such that the contribution of molecular diffusion can be neglected [4]. Furthermore, to quantify the presence of the tracer in the pore structure of the aquifer, the scalar field of mass concentration c is introduced. In such a case, in each point of the flow domain, the mass concentration c is defined as

$$c = \lim_{\Delta V \to 0} \frac{\Delta m}{\Delta V}, \qquad (1)$$

in which Δm denotes the tracer mass contained in a volume ΔV. As is evident, the given definition (1) assumes the validity of continuum mechanics i.e. the representation of micro quantity on macro scale by an averaging process inside the porous material contained in the *representative elementary volume* [2]. As a consequence of spatial averaging, the local irregular pore structure, which evidently affects the convective transport of a tracer, is described on the macroscopic scale of observation by introducing the dispersive component of the transport [1, 2]. Before considering the experimental observations of trace transport in a dedicatedly constructed model, it is opportune to introduce the basic theoretical description of the considered phenomena.

2 Convective-dispersive transport

Before introducing some basic aspects of transport processes in porous materials, note that the author's intention is to compare the experimentally measured temporal variation of the mass concentration c with the one obtained by the one-dimensional and two-dimensional analytical solution of the governing differential equation [5]. For that reason, the 3D flow field inside the physical model should be manipulated in such a way that it can be classified as uniform (at least on a spatial segment of a flow domain). In other words, the flow field in the

*Corresponding author. Tel.: + 385 51 265 900; fax: + 385 51 265 910
e-mail address: vanja.travas@gradri.hr

physical model should meet the condition $\partial v/\partial x=0$, where the x coordinate direction is parallel with the flow direction. The mentioned coincides with the assumption under which the analytical solutions of the governing differential equation are derived. Apart from this condition, the considered analytical solutions are derived under the assumption that the porous material is homogenous and isotropic [5]. Under all these circumstances, and for a transport process characterized by the dominant influence of convection, the governing differential equation for a two-dimensional case, and in a plane perpendicular to the gravity force, takes the form

$$\frac{\partial c}{\partial t}+\frac{v}{R}\frac{\partial c}{\partial x}=\frac{D_L}{R}\frac{\partial^2 c}{\partial x^2}+\frac{D_T}{R}\frac{\partial^2 c}{\partial y^2}-\lambda c, \qquad (2)$$

and the same equation for 1D is obtained by excluding the second term on the RHS, generating

$$\frac{\partial c}{\partial t}+\frac{v}{R}\frac{\partial c}{\partial x}=\frac{D_L}{R}\frac{\partial^2 c}{\partial x^2}-\lambda c, \qquad (3)$$

in which v denotes the water flow velocity [L/T], D_L denotes the coefficient of longitudinal dispersion [L^2/T], D_T denotes the coefficient of transverse dispersion [L^2/T], R denotes the coefficient of retardation [1] and λ denotes the coefficient of tracer mass degradation [T^{-1}]. For an aquifer with effective porosity n_e [5] and constant geometrical characteristic such as height m and width w, the case of instant injection of a tracer with mass ΔM is considered. This kind of initial condition can be defined as

$$c(x=0,y=0,t=0)=\frac{\Delta M}{n_e m R}\delta(x)\delta(y), \qquad (4)$$

for a 2D case and

$$c(x=0,t=0)=\frac{\Delta M}{n_e m w}\delta(x), \qquad (5)$$

for a 1D case in which $\delta(x)$ denotes the Dirac delta function defined as

$$\delta(x)=\begin{cases}1 & if \quad x=0\\ 0 & if \quad x\neq 0\end{cases}. \qquad (6)$$

Since the analytical solutions of (2,3) assumes an imaginary infinite aquifer, the boundary conditions are defined as

$$c(\pm\infty,\pm\infty,t)=0, \qquad (7)$$

and

$$c(\pm\infty,t)=0. \qquad (8)$$

According to the given assumptions, boundary and initial conditions, (2) produces a function $c(x,y,t)$ and (3) produces a function $c(x,t)$ that defines the spatial distribution of tracer mass concentration c in an instant of time t. Note that the spatial distribution is given along the streamline at which the tracer was injected. The procedure to retrieve the solution can be found in the literature [5] and leads to

$$c(x,y,t)=\frac{\Delta M}{4\pi n_e m v_d\sqrt{\alpha_L\alpha_T t}}e^{-\frac{(x-vt/R)^2}{4\alpha_L vt/R}-\frac{y^2}{4\alpha_L vt/R}}e^{-\lambda t}. \qquad (9)$$

for a 1D case and to

$$c(x,t)=\frac{\Delta M}{2wmn_eR\sqrt{\frac{\pi\alpha_L vt}{R}}}e^{-\frac{(x-vt/R)^2}{4\alpha_L vt/R}}e^{-\lambda t}. \qquad (10)$$

for a 1D case. To make the comparison between the theory (9, 10) and experiment valid, it should be noted that the physical model must ensure such flow conditions that will be coherent with the introduced assumptions. Also, the experiments should be run with the same initial (4, 5) and boundary conditions (7,8). Therefore, the briefly given theoretical consideration was necessary to appreciate the process of planning the experiments, which are hereafter presented.

3 Physical model

To obtain the needed functional requirements, it is concluded that the physical model should contain four sections; that are: (i) the working section filled with porous material and located between the (ii) *pump chamber* and the (iii) *spillway chamber*, and

the (iv) *volumetric chamber*. All the sections and their relative positions are illustrated in Fig. 1 [6].

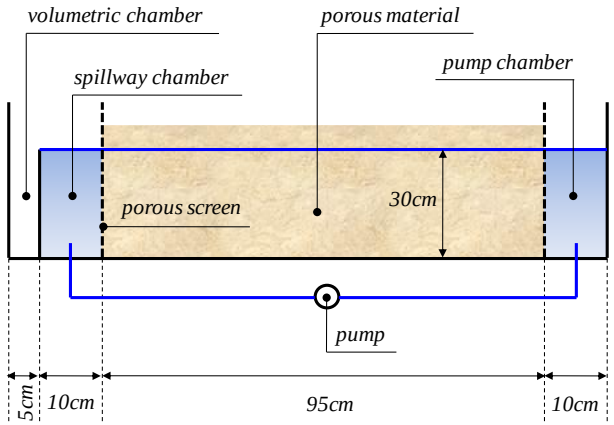

Figure 1. The cross section of the physical model.

To generate the pressure gradient between the pump chamber and the spillway chamber (Fig. 1), which will consequently induce the flow through the porous material, an external pump is used to obtain water circulation between these two regions.

Before considering the case of tracer injection and its transport with the water flow inside the porous material, note that the analytical solution (9, 10) of the same physical process will require the velocity v of the flow. For this reason, the physical model should be firstly used to identify the saturated hydraulic permeability K of the contained porous material. Namely (by knowing K), the flow velocity v can be defined through the Darcy's law

$$v_d = K I_E \,, \tag{11}$$

in which v_d is the Darcy velocity (not actual velocity in the porous material) and I_E is the non-dimensional parameter (i.e. the slope of an energy line) defined as

$$I_E = \frac{\Delta L}{\Delta h} \,. \tag{12}$$

For the considered system (Fig. 1), ΔL denotes the distance between the pump and the spillway chamber and Δh denotes the difference in water level h between the same chambers. By knowing the Darcy velocity v_d (11), the actual velocity v can be computed as [1, 3]

$$v = \frac{v_d}{n_e} \,. \tag{13}$$

Few measurements performed on different samples reveal that the effective porosity n_e of the used porous material is equal to 0.516. As a consequence, the actual velocity v (13) is twice the Darcy velocity v_d (11). From all mentioned, it is evident that the velocity v, which is needed in (9, 10), can be determined only by knowing v_d. For this purpose, note that the geometrical relationship in (12) can be easily measured. In other words; to compute the actual velocity v from (13), the saturated permeability K must be defined.

3.1 Determination of saturated permeability K

For any porous material, the saturated permeability K cannot be measured directly (K can only be computed from a known relationship between other basic SI physical quantities that can be directly measured). In other words, since it is a part of a constitutive description of the material (7), its value can only be computed from a predefined functional relationship. Particularly, as the discharge Q is given as the product of the cross section area A of the porous material and Darcy's velocity v_d, it follows from (11) that the saturated permeability K can be computed as

$$K = \frac{Q}{A}\frac{\Delta L}{\Delta h} \,. \tag{14}$$

Note that apart from the discharge Q, all the other terms in (14) are geometrical properties of the flow and can be determined by using simple measurements of the distance between particular points. However, to compute K from (14), the flow should be steady to ensure that the geometrical relations do not change in time. For the constructed physical model, a steady flow field and the related geometrical properties are illustrated in Fig. 2.

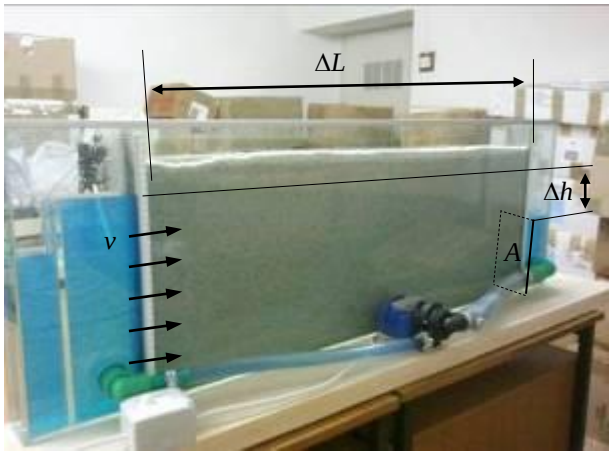

Figure 2. Photograph of the physical model with the notations for a few geometrical quantities.

It is also important to note that the computation of K through (14) assumes that the porous material in the physical model is homogenous and isotropic. For this purpose, homogenous sand is used (with a uniform distribution of granular fractions between 2 and 3 mm). The used sand can also be treated as isotropic porous material (from the statistical point of view), which is deduced qualitatively by a visual inspection of the contained grains. In other words, the shape of the contained grains is nearly spherical, meaning that the grains will provide the same resistance in any direction of the flow.

Resuming, the computation of K obviously requires the measurement of Q (14). A volumetric chamber (Fig. 1) is used for this purpose and the methodology to obtain Q is shortly discussed hereafter.

3.2 Flow measurement

The discharge Q (which is defined as $\Delta V/\Delta t$) is measured volumetrically [6], i.e. by measuring a particular volume of water ΔV in a time interval Δt.
For this purpose, the physical model contains the *volumetric chamber* (Fig. 1). To illustrate the related procedure and the role of the chamber, a set of illustrations is given in Fig. 3.
It is important to note that at the beginning of the experiment the volumetric chamber is empty and the other two chambers are completely filled with water (Fig. 3a).
It is opportune to exclude the influence of the pump $Q(h)$ curve and introduce the valid assumption that the pumping rate Q is constant in time.

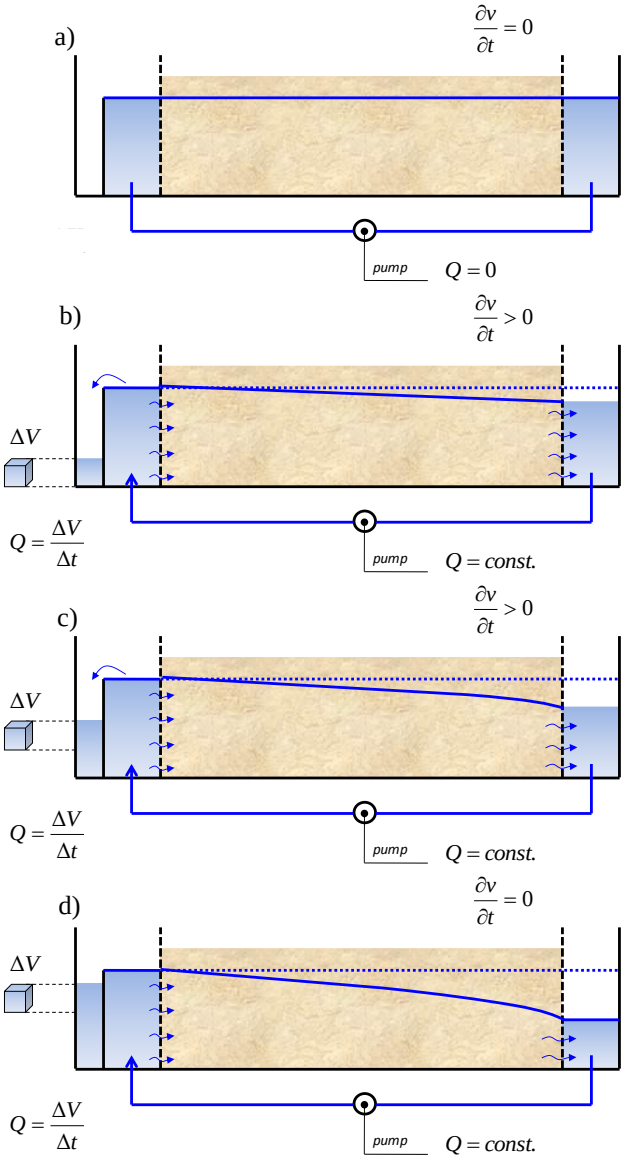

Figure 3. Illustrations of water level: a) standstill configuration to d) steady flow conditions ($\partial v/\partial t=0$).

Strictly speaking, the pumping rate is not constant and this is due to the fact that the flow rate of every pump is dependent on the water pressure (h_p) at which the pump works [6]. Namely, from the beginning of the experiment (Fig. 3a) to the reached steady flow field (Fig. 3d), the water level h_p in the pump chamber decreased in time. Theoretically, this will imply the successive increasing in Q. However, in order to establish this difference, the pump had to be supplied with different voltage for the purpose of inducing a few different steady flow fields.

For each of them, the increase in water level in the volumetric chamber was carefully measured. In each case it was confirmed that the working range Δh was small enough so that Q can be assumed as constant in time (Fig. 4).

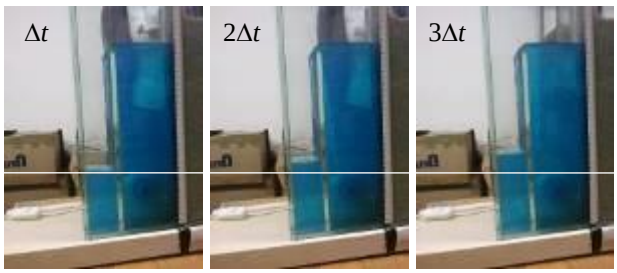

Figure 4. A set of photographs taken in equidistant time intervals to illustrate the constant raising of water level inside the volumetric chamber.

As the dispositions of the chambers and the pump suggest (Fig. 1), the activation of the pump in the initial-standstill configuration (Fig. 3a) will cause a decrease in the water level in the pump chamber (Fig. 3b) simultaneously increasing the level in the spillway chamber. As the spillway chamber was previously filled to its top (Fig. 3a), the pumped water will start to fulfill the volumetric chamber (Fig. 3b).

Under the assumption that the pumping rate Q is constant, there would be also a constant rise of the volume of the water in the volumetric chamber. Once the pumping rate becomes equal to the inflow rate from the spillway chamber into the porous material (Fig. 3d), the steady flow conditions are reached. As a consequence, the water levels in each chamber remain constant in time, and the discharge Q can be as the water volume ΔV in the volumetric chamber divided by a time Δt needed to reach the steady flow conditions.

Note that even the pumping flow rate is constant in time; the discharge in the physical model varies due to the progressive increasing in the hydraulic gradient near the pump chamber (increasing in velocity according to 11). However, once the steady flow condition is reached, the flow rate in the physical model and the pump coincides. Since the water level doesn't change in time under steady flow conditions, and under the assumption that the pumping rate is constant, the water extracted from the model and transported to the volumetric chamber divided by the time needed to extract it from the model, represents the discharge in the physical model, an average value being defined as $\Delta V/\Delta t$. Also, it is worth noting that the variations in discharging in the physical model taking place during the time in which the steady flow conditions are reached are not of interest.

Congruently with the above mentioned, the discharge Q in the model was indentified to be 19.94 cm^3/s. The obtained steady flow field results in a water level h_p=15.8 cm in the pump chamber. Since the water level h_s in the spillway chamber is always constant (30 cm), the difference in water levels Δh was 14.2 cm, which finally through (14) defines the saturated permeability K=1.64 cm/s [6]. A few experiments with different pumping rate confirm these measurements.

4 Analysis of the flow field

The comparative study between the measurements and theoretical predictions will be justified only if the flow field in the physical model is congruent with the assumptions used to retrieve the analytical solutions of the governing differential equations. Since the analytical solution is derived for 1D and 2D transport processes, it is required to identify a stream line inside the physical model along which the velocity vector doesn't change considerably. For this purpose, note that the flow field in the physical model can be treated as a potential flow [1] and that the net of streamlines can be reconstructed by knowing the free stream line at the top boundary of the flow field (i.e. phreatic surface). The mentioned follows from the fact that the flow field is steady and the flow domain will be completely defined by knowing the free boundary. Accordantly, the free streamline can be obtained by integrating the 1D Laplace equation [4], which for homogenous and isotropic porous materials can be written as

$$\frac{d}{dx}\left(h(x)\frac{dh}{dx}\right)=0\,, \tag{15}$$

in which the dependent variable h is the water level along the coordinated x (which increases in the flow direction). By double integration of (15), it follows that

$$h^2(x) = C_1 x + C_2 \,, \tag{16}$$

in which C_1 and C_2 are integration constants obtained from the known boundary conditions [6], which are the water level h_1 at the upstream side and the water level h_2 at the downstream side of the model. So, the condition at the upstream side where x=0, is that h=h_1, from where it can be obtained that C_2 is equal to $(h_1)^2$. On the other side (Figure 2), i.e. at the downstream boundary where x=ΔL, h=h_2, it follows that C_1= $(h_2)^2$ – $(h_1)^2\Delta L$. By inserting the computed constants C_1 and C_2 in (16), the analytical solution of (15) defines the water level $h(x)$ in each coordinate x as

$$h(x) = \sqrt{h_1^2 - (h_1^2 - h_2^2)\frac{x}{\Delta L}} \,. \tag{17}$$

For the flow field in the physical model, which is defined by h_1=h_s=30 cm and h_2=h_p=15.8 cm, the free stream line (17) and a set of ten equidistant stream lines are illustrated in Fig. 5.

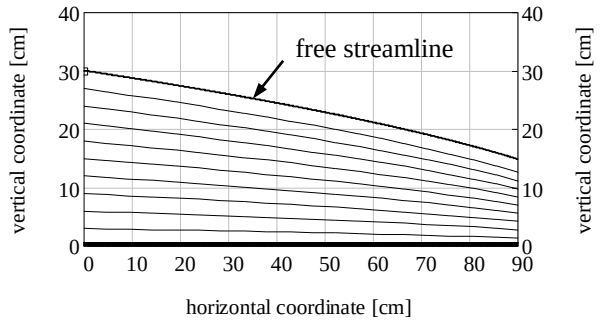

Figure 5. Analytical solution of the free streamline.

To compare the analytical solution (17) with the flow field inside the physical model, 4 streamlines were visualized with dye injections. The dye was injected near the spillway chamber, at four different heights, and at different times due to the fact that the simultaneous injection was very hard to obtain. As a consequence, the dyes were shifted vertically and horizontally. The observations were recorded with photographs and presented together with the analytical solution in Fig. 6.

Firstly, it is worth mentioning that in a steady flow field, as the one in the physical model, the trajectory of fluid particles will coincide with the streamlines. As can be noted (Fig. 6), the dyes trajectory coincides with the related streamlines predicted by the theory (17). However, the location of the free stream line was not exactly predicted. Namely, as illustrated in Fig. 6, the free stream line in the physical model is slightly moved above the solution of the equation (15). The origin of this difference is the capillary rising of water in porous materials. The empirical quantification of capillary rising, known from the literature [3], predicts the difference of 1cm, which was also evidenced in the physical model.

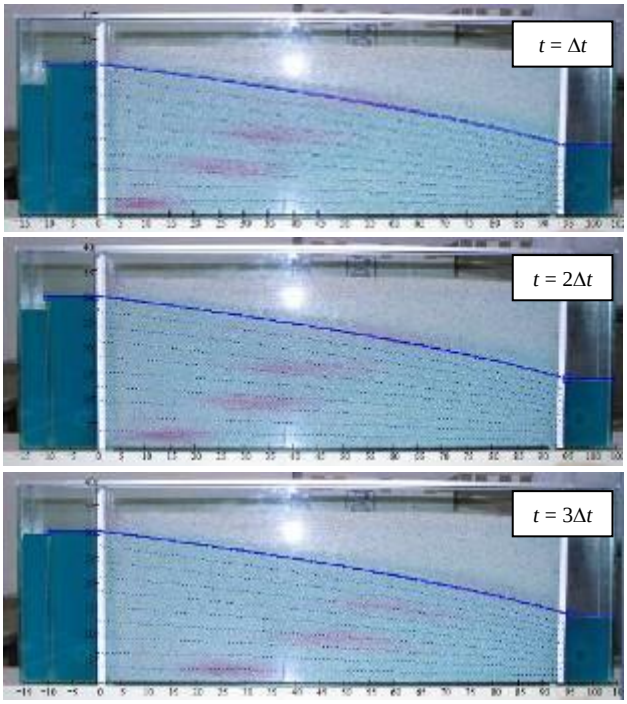

Figure 6. Set of photographs taken in equidistant time instants after the dyes were injected.

Since the flow is steady and the curved free streamline reveals the presence of vertical component v_y of velocity vectors **v**, the horizontal component v_x will also vary along the physical model. So, to perform a comparative analysis between the analytical solutions (9, 10) and measurements, an appropriated streamline on which the tracer will move with a constant velocity v should be found. For this purpose, and due to the steady flow ($\partial Q/\partial t$=0), the increase in flow velocity v can be quantified as a consequence of the decrease in water level h (Fig. 5). Although the change in v_x will not be the same for different streamlines, the change in $v_x(x)$ obtained through Q=$v_xA(h)$ can be interpreted as an average velocity component. Therefore, under the assumption that the magnitude of the velocity component v_y could be neglected (in comparison

with the v_x component), Fig. 7 illustrates the velocity distribution along the physical model.

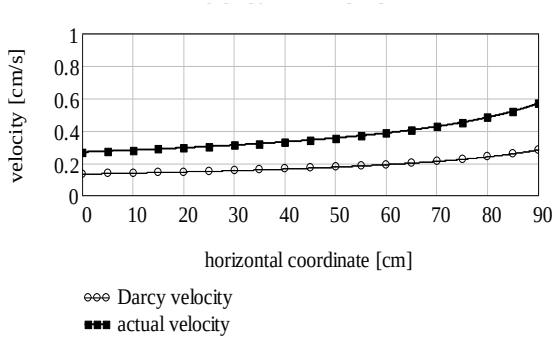

Figure 7. Spatial distribution of Darcy's velocity v_d and the actual velocity v along the physical model.

As Fig. 7 shows, the actual velocity v_x i.e. v changes almost twice between the spillway and the pump chamber (Fig. 1). However, it is worth noting that there is a rapid increase in v at the end of the physical model. On the other hand, between the coordinates x=0 and x≈40 cm, the change in v is negligible. In other words, the flow path between these two coordinates can be used to perform the comparative analysis, as is illustrated hereafter.

5 Dye injection and transport

To meet the initial condition (4, 5), the tracer mass ΔM should be injected instantaneously as the analytical solution (9, 10) has suggested. To approach this theoretical condition (as much as possible), the tracer mass was injected with a relatively tight tube (piezometer). So, the dye injection may be considered as point phenomena in a very small period of time. A few photographs of a sequence of dye injection are given in Fig. 8. After ~ 0.5 sec, the entire tracer contained in the tube was omitted in the flow field.

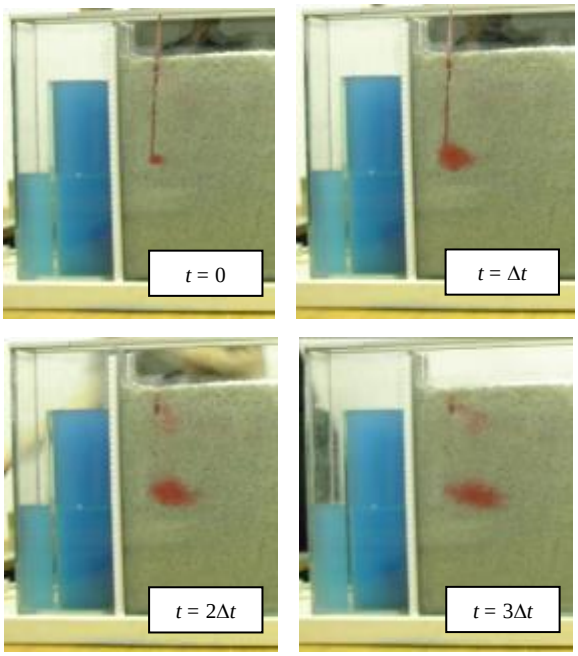

Figure 8. A sequence of photographs taken after the dye injection in the porous material.

Since the mass concentration c is always measured indirectly by measuring the electrical conductivity S (mS/cm), to increase the initial very small electrical conductivity and enable the measurements of S, the tracer has been previously salted. Under constant pressure and temperature, the relation between the mass concentration and the measured electrical conductivity S is generally linear, and is given as c=0.67S [7] in which the mass concentration c is expressed in mg/l and the electrical conductivity S in μS/cm.

It is worth mentioning that the tracer (dye) and the water in the physical model already posses initial electrical conductivity S. Thus, to measure only the increase in electrical conductivity ΔS and to relate it to the previously measured mass of a tracer ΔM (4, 5), the initial value of S has been recorded and used as a reference value in these measurements. To relate only the mass ΔM with the mass concentration c (9,10), the electrical conductivity of the tracer has been previously significantly increased by adding a salt with mass ΔM_s. In this case, in any region inside the porous material the electrical conductivity S of a contained water will be proportional to the solution mass $M_t=\Delta M+\Delta M_s$.

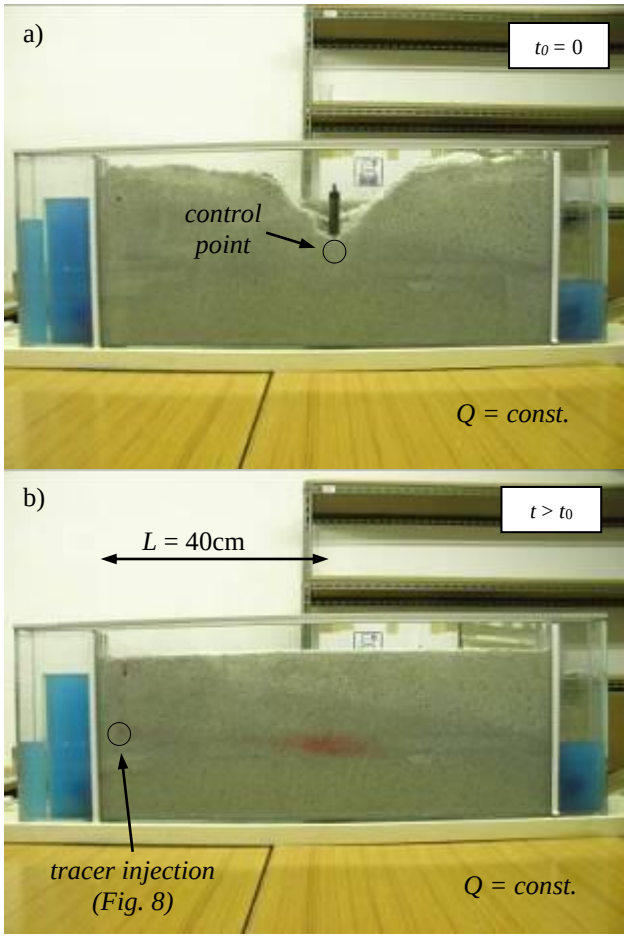

Figure 9. Photographs of a) DIVER position in the porous material and b) tracer path.

To measure and record the change in electrical conductivity ΔS, a CTD Diver [8] is used and if the dimensions of the probe are to be considered, the Ion-Selective probes can be regarded as an alternative. The Diver position, i.e. the control point at which the change ΔS is recorded, is selected so that between the point of injection of a dye and the measured point of the flow velocity doesn't change significantly, as is illustrated in Fig. 9.

To compute the change in mass concentration (9, 10) at the same point at which ΔS was measured (Fig. 9), the coefficient of retardation R and the coefficient of longitudinal dispersion D_L should be known in advance (note that for a two-dimensional case, the coefficient of transverse dispersion α_T can be obtained as $\alpha_L/10$ which is a regular relationship evidenced by measurements in aquifers [1, 3]). For this purpose, a few experiments were performed to estimate their quantity. For all cases, relative to the velocity of the contained water, it was concluded that the used porous material doesn't provide an evident retardation in a tracer flow. In other words, the retardation coefficient is estimated to be R~1. On the other hand, a measurement of the longitudinal stretching of the tracer plum between the point of entrance in the porous material and the control point (Fig. 9) indicates that the coefficient of longitudinal dispersivity α_L is around 0.1 cm, which defines α_T as close to 0.01 cm. Namely, α_L defines the coefficient of longitudinal dispersion as $D_L = v\,\alpha_L$ [1, 9].

It should be also emphasized that for a dominant convective transport, as the one being realized in the physical model (Fig. 9), the transversal dispersion D_T is always smaller than D_L. With reference to the flow conditions achieved in the physical model, α_T was indentified to be at least ten times smaller than the longitudinal dispersion, which is in accordance with the mentioned experimental but also *in-situ* measurements. The measured and theoretically predicted variations of the mass concentration c at the control point are presented in Fig. 10.

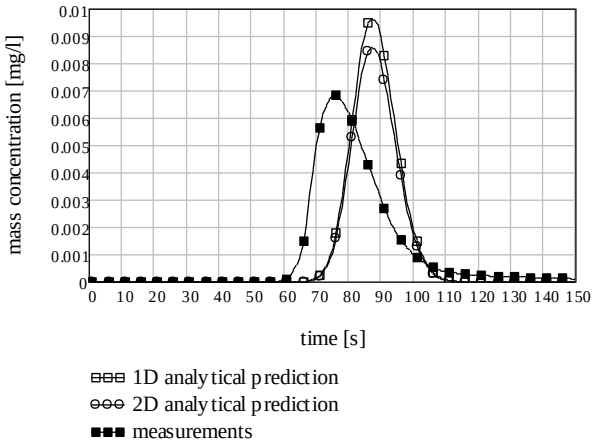

Figure 10. The measured and predicted time variations of mass concentration.

The maximal predicted value of mass concentration with the 1D theoretical model is about 20% greater than the measured one (Fig. 10). This difference arises from the small but still present transversal component of dispersivity (D_T), which spreads the traces around the region at which the Diver was positioned (Fig. 9). On the other hand, due to the extra dimension, the 2D analytical model enables the spreading of the salt in a plane perpendicular to the gravity force which consequently gives better

results by reducing the peak mass concentration (Fig. 9). Correspondingly, it can be concluded, as expected, that the 3D analytical solution will give even better results.

The difference in the area below the curves is the tracer mass, which was not detected because it was above and below the Diver. However, if the wideness of the curves is considered (Fig. 10), it follows that the longitudinal dispersion D_L has been correctly predicted, which can be supported by the fact that the span of the curves is about the same. Taking into account the time at which the mass M_t reaches the position in which the mass concentration has been measured and calculated, it can be seen that in such a case of a physical model, the increase in c has started before the theory predicts. However, the difference is again relatively small and can be referred to the still small change in velocity along the streamline at which the tracer was injected. Namely, as Fig. 7 shows, the horizontal velocity increases as the flow approaches the other side of the physical model, i.e. it is not exactly the same as the analytical solution (9, 10) requires. Interesting enough, the measured variation in mass concentration is not symmetrical as it should be. This observation can be understood provided that Diver geometry has been considered. Namely, the sensor which measures the electrical conductivity is placed at the bottom of the Diver in a chamber that is only opened on one side. The Diver is placed in the way that the open side of a chamber faces the direction of the flow. Considering the local flow field, this orientation of a one side open chamber will briefly retain the tracer and release it gradually with the constantly supplied clean water. The difference in time needed to enter and leave the chamber manifests itself as the asymmetrical temporal variation in c (Fig. 10).

6 Concluding remarks

A physical model for tracer transport inside an intergranular porous material has been elaborated. To obtain the essential ingredient of objectivity for all measurements, the physical model constructed with the intention of controlling the flow parameters. For this purpose, i.e. to check (for the purpose of checking) whether the intention was achieved, the 1D and 2D analytical solutions of a related governing differential equation for mass transport in porous media was used to compare whether the theoretically predicted temporal variation of the mass concentration c is in accordance with the measured one at the same point in the flow domain. Namely, for this purpose, it was necessary to control the flow field inside the physical model so that the assumptions under which the analytical solution is retrieved can be valid. Except small discordance in values, arising from a previously discussed known origin, the tracer transport is shown to be qualitatively and quantitatively the same as the one predicted by theory. However, the 2D analytical solution, as expected, gives better results than the 1D model, i.e. it shows a better agreement with the measured data. This is due to the fact that the 2D analytical model introduces the possibility of spreading the salt in the plane perpendicular to the gravity force, reducing thus the peak mass concentration. Undoubtedly, both analytical solutions predict too much salt (about 20%) at the measured point and this is due to the fact that the possibility of spreading the salt is reduced by reducing the dimensionality of the flow field. Accordingly, the 3D analytical solution will give even better results because it includes the spreading of the salt in the vertical direction. According to all the mentioned, it can be concluded that the flow field inside the physical model can be controlled. However, due to the geometry of the flow i.e. the width of the working section of the physical model, the used Diver cannot be recommended for further measurements, given the fact that the local flow field around the Diver is significantly influenced by its presence (Fig. 10). However, we can conclude that in case the dimensions of the probe are taken into consideration, the Ion-Selective probes can be regarded as an alternative to the CTD Diver.

References

[1] Bear, J., Bachmat, Y.: *Theory and Applications of Transport in Porous Media – Introduction to Modeling of Transport Phenomena in Porous Media*, Published by Kluwer Academic Publisher, The Netherlands, 1990.

[2] Bear, J.: *Hydraulics of Groundwater*, New York: McGraw-Hill, 1979.

[3] Bear, J., Buchlin, J-M.: *Theory and Applications of Transport in Porous Media - Modelling and Applications of Transport*

Phenomena in Porous Media, Published by Kluwer Academic Publisher, The Netherlands, 1991.

[4] Chesnaux, R., Molson, J.W., Chapuis, R.P.: *An Analytical Solution for Ground Water Transit Time through Unconfined Aquifers*, Geological and Mining Engineering, P.O. Box 6079 Station Centre-ville, Montreal, Quebec Canada H3C 3A7, 2004.

[5] Kinzelbach, W.: *Numerische Methoden zur Modellierung des Transportes von Schadstoffen im Grundwasser*, Oldenbourg, Munich, 1992.

[6] Rubeša, A.: *Physical model of convective-dispersive transport in granular porous media*, Graduated Engineer Thesis, Faculty of civil engineering University of Rijeka, Rijeka, 2011.

[7] Fofonoff, N.P., Millard, R.C.: *Algorithms for computation of fundamental properties of seawater*, Unesco/SCOR/ICES/IAPSO Joint Panel on Oceanographic Tables and Standards and SCOR Working Group 51, 1983.

[8] Schlumberger Water Services, Technology Sheet, CTD-Diver, Groundwater monitoring for Diverse environments, March 2010.

[9] Zou, S. and Parr, A.: *Estimation of dispersion parameters for two-dimensional plumes*, Groundwater, 31 (1993) 3.